

## Non peer-reviewed preprint submitted to EarthArXiv

---

This manuscript is a preprint and has been submitted for publication in *Frontiers in Marine Science - Ocean Observations*. Subsequent versions of this manuscript may have slightly different content. If accepted, the final version of this manuscript will be available via the “Peer-reviewed Publication DOI” link on the right-hand side of this webpage. Please feel free to contact the authors.

We welcome your feedback.

---

### **Eavesdropping at the speed of light: distributed acoustic sensing of baleen whales in the Arctic**

Léa Bouffaut<sup>1\*</sup>, Kittinat Taweessintananon<sup>1,2</sup>, Hannah J. Kriesell<sup>1</sup>, Robin A. Rørstadbotnen<sup>1</sup>, John R. Potter<sup>1</sup>, Martin Landrø<sup>1</sup>, Ståle E. Johansen<sup>3</sup>, Jan K. Brenne<sup>4</sup>, Aksel Haukanes<sup>4</sup>, Olaf Schjelderup<sup>5</sup> and Frode Storvik<sup>5</sup>

<sup>1</sup> Acoustics Group, Department of Electronic Systems, Norwegian University of Science and Technology (NTNU), Trondheim, Norway

<sup>2</sup> PTT Exploration and Production Public Company Limited, Bangkok, Thailand

<sup>3</sup> Department of Geoscience and Petroleum, Norwegian University of Science and Technology (NTNU), Trondheim, Norway

<sup>4</sup> Alcatel Submarine Networks Norway AS, Tiller, Norway

<sup>5</sup> Uninett AS, Trondheim, Norway

\*Corresponding author: Léa Bouffaut [lea.bouffaut@cornell.edu](mailto:lea.bouffaut@cornell.edu)

1 Eavesdropping at the speed of light: distributed acoustic sensing  
2 of baleen whales in the Arctic

3 Léa Bouffaut<sup>\*1</sup>, Kittinat Taweessintanon<sup>1,2</sup>, Hannah J. Kriesell<sup>1</sup>, Robin A.  
4 Rørstadbotnen<sup>1</sup>, John R. Potter<sup>1</sup>, Martin Landrø<sup>1</sup>, Ståle E. Johansen<sup>3</sup>, Jan K. Brenne<sup>4</sup>,  
5 Aksel Haukanes<sup>4</sup>, Olaf Schjelderup<sup>5</sup>, and Frode Storvik<sup>5</sup>

6 <sup>\*</sup>Corresponding author: lea.bouffaut@cornell.edu

7 <sup>1</sup>Acoustics Group, Department of Electronic Systems, Norwegian University of Science  
8 and Technology (NTNU), NO-7491 Trondheim, Norway

9 <sup>2</sup>PTT Exploration and Production Public Company Limited, Bangkok 10900, Thailand

10 <sup>3</sup>Department of Geoscience and Petroleum, Norwegian University of Science and  
11 Technology (NTNU), NO-7491 Trondheim, Norway

12 <sup>4</sup>Alcatel Submarine Networks Norway AS, Vestre Rosten 77, Tiller, 7075, Norway

13 <sup>5</sup>Uninett AS, Abels gate 5, Trondheim, 7030, Norway

14 March 20, 2022

15 **Keypoints:**

- 16 • This is the first case of wildlife monitoring using Distributed Acoustic Sensing (DAS).  
17 • DAS has the ability to record and localize vocalizing baleen whales in 3D and so to provide fully  
18 passive conventional seismic records.

19 **Abstract**

20 In a post-industrial whaling world, flagship and charismatic baleen whale species are indicators of  
21 the health of our oceans. However, traditional monitoring methods provide spatially and temporally  
22 undersampled data to evaluate and mitigate the impacts of increasing climatic and anthropogenic  
23 pressures for conservation. Here we present the first case of wildlife monitoring using distributed  
24 acoustic sensing (DAS). By repurposing the globally-available infrastructure of sub-sea telecommuni-  
25 cation fiber optic (FO) cables, DAS can (1) record vocalizing baleen whales along a 120 km FO cable  
26 with a sensing point every 4 m, from a protected fjord area out to the open ocean; (2) estimate the 3D

27 position of a vocalizing whale for animal density estimation; and (3) exploit whale non-stereotyped  
28 vocalizations to provide fully-passive conventional seismic records for subsurface exploration. This  
29 first example’s success in the Arctic suggests DAS’s potential for real-time and low-cost monitoring  
30 of whales worldwide with unprecedented coverage and spatial resolution.

31 **Keywords:** Distributed acoustic sensing, bioacoustics, Passive acoustic monitoring, Baleen whales,  
32 Cetacean conservation, Blue whale, Fin whale.

### 34 Plain Language Summary

35 Slowly recovering from industrial whaling, large whales such as blue and fin whales are considered  
36 threatened or critically endangered. Simultaneously, they face climate change and the augmentation  
37 of human maritime activities. Their conservation requires global and reliable monitoring efforts.  
38 Using whale sounds to study habitat use, map migration patterns, assess stock, evaluate and mitigate  
39 human impacts is a well-established practice. However, because dedicated acoustic recorders are  
40 relatively costly to deploy and maintain, they are still sparse, causing spatial and temporal monitoring  
41 gaps.

42 Taking roots in an experiment conducted at the doorstep of the Arctic, we introduce distributed  
43 acoustic sensing (DAS) for wildlife monitoring. This technology converts already-set fiber optic  
44 telecommunication cables into ultra-long acoustic arrays without additional infrastructure costs. We  
45 recorded data along 120 km of fiber optic cable, with a sensing point every 4 m. Here, we demonstrate  
46 the possibility to record, detect, localize and track large whale sounds using DAS. Furthermore,  
47 we show that the array’s unique spatial resolution enables new applications such as under-seafloor  
48 imaging using a single whale call.

49 More than 1.2 million km of fiber-optic cables are installed all over the world’s oceans. Converted  
50 into DAS, it has the potential to revolutionize acoustic-based marine mammal conservation.

## 51 1 Introduction

52 While slowly recovering from industrial whaling, many baleen whale species (*Mysticeti*) [5] are still  
53 threatened or critically endangered [23]. Simultaneously, these animals and their vast ocean habitat are  
54 subject to an increasing number of stressors driven directly or indirectly by anthropogenic activities,  
55 e.g., entanglement in fishing gear, ship strikes and noise pollution associated with the global increase of  
56 ship traffic. Additionally, alteration of water and nutrient cycles by plastic and chemical pollution affect  
57 the entire food webs [51]. Climate change has further forced cetaceans to adapt their migration routes  
58 (or their timing). Globally, many species shift poleward to their preferred sea-surface temperature [53].

59 In the Arctic, the climate is changing faster than anywhere else in the world. This has been linked to  
60 major shifts in species distributions related to sea-ice loss and the Atlantification of the region [18]. In  
61 the high latitudes of the Svalbard archipelago, boreal species e.g., blue whales (*balaenoptera musculus*),

62 fin whales (*balaenoptera physalus*), humpback (*megaptera novaeangliae*) and sei whales (*balaenoptera*  
63 *borealis*), have been considered seasonal residents, traditionally present from late spring/early summer  
64 to the autumn and spending their winters at lower latitudes [36]. Recently however, fin whales have  
65 been observed year-round [26, 31]. Furthermore, with sea ice-loss came an increase in human activities.  
66 While ship traffic is already abundant between the Barents and North sea and Svalbard [16, 43], it will  
67 likely intensify in species rich areas [18] with the new cross-Arctic shipping routes [37]. Airgun signals  
68 can already be recorded all-year round close by, in the western Fram Strait [1]. It is urgent to establish a  
69 baseline of the environment’s exposure and marine mammal vulnerability to these anthropogenic stressors  
70 to mitigate their impacts, which requires first, monitoring.

71 From fixed autonomous archival recorders to moving near-real-time multi-sensory platforms [6, 35],  
72 passive acoustic monitoring has proven to be a reliable and suitable mean for baleen whale studies  
73 [21]. However, it is still relatively expensive to deploy conservation-focused hydrophones and despite the  
74 research community’s global efforts and the exponentially increasing amount of data collected world-wide  
75 [27], recorders are sparse and unevenly spread: the oceans are under-sampled [1, 2, 16, 18].

76 Meanwhile, Distributed Acoustic Sensing (DAS) has started to conquer many fields both at sea [20]  
77 and on land [41], with exponential progresses in terms of data quality, spatial coverage and bandwidth  
78 [41, 54]. Using an interrogator, DAS technology re-purposes existing dark fiber optic (FO) cables to  
79 record nano strain [14] and has the potential for real-time monitoring over hundreds of kilometers with a  
80 spatial resolution of a few meters [17, 54]. Initially applied to geophysical data collection [15, 20, 41, 47],  
81 DAS has recently aroused interest with waterborne sound sources, e.g., near-surface ship detection and  
82 bearing in the Mediterranean sea [44] and, data quality assessment using controlled airguns sources  
83 compared to ocean bottom seismometers recordings in Japan [32] and with seismic streamers in Norway  
84 [50] showed similar capabilities in terms of frequency response and signal to noise ratio (SNR). This  
85 article demonstrates the untapped potential of DAS for baleen whale monitoring.

86 Data was acquired during summer 2020 around Isfjorden, Svalbard, Norway, at the doorstep of the  
87 Arctic (Fig. 1). At that time of the year, sighting and a previous acoustic study around the archipelago  
88 demonstrate the consistent presence of blue, fin and humpback whales, and possible presence of sei whales  
89 [2, 18, 38]. Data used in this work is available [9].

## 90 **2 Results and Discussions**

### 91 **2.1 Experimental Setup**

92 We re-purposed a dark fiber (SMF-28 single mode silica), i.e. a spare fiber in an existing Uninett subma-  
93 rine telecommunication cable connecting Longyearbyen to Ny-Ålesund in Svalbard, Norway (Fig. 1 (a)).  
94 To minimize the cost of installation, it is common practice to lay spare fibers in communication ca-

bles. The fiber, trenched 1 to 2 m into soft sediment, followed the seafloor bathymetric variations. The Longyearbyen end of this cable was connected to an Alcatel Submarine Networks OptoDAS interrogator. The interrogator injects linear frequency-modulated optical pulses which are back-scattered by anomalies in the fiber [54]. Then, for each sampled position along the fiber, further named channels, it calculates the time-differentiated phase change of the back-scattered response from consecutive sweeps over a section of the fiber, indicated by the gauge length. The delay is converted into longitudinal strain for the corresponding fiber section [19]. Normal signal decay along the fiber 0.2 dB/km. The maximum length of fiber  $L$  that can be converted to DAS is mostly constrained by the chosen sampling frequency  $f_s$  such as  $L = \frac{c}{2nf_s}$ , with  $c = 299792458$  m/s the speed of light in the fiber and  $n = 1.4667$  the group refractive index of the fiber. For example, more than 9 km can be converted to DAS if  $f_s = 10$  kHz.

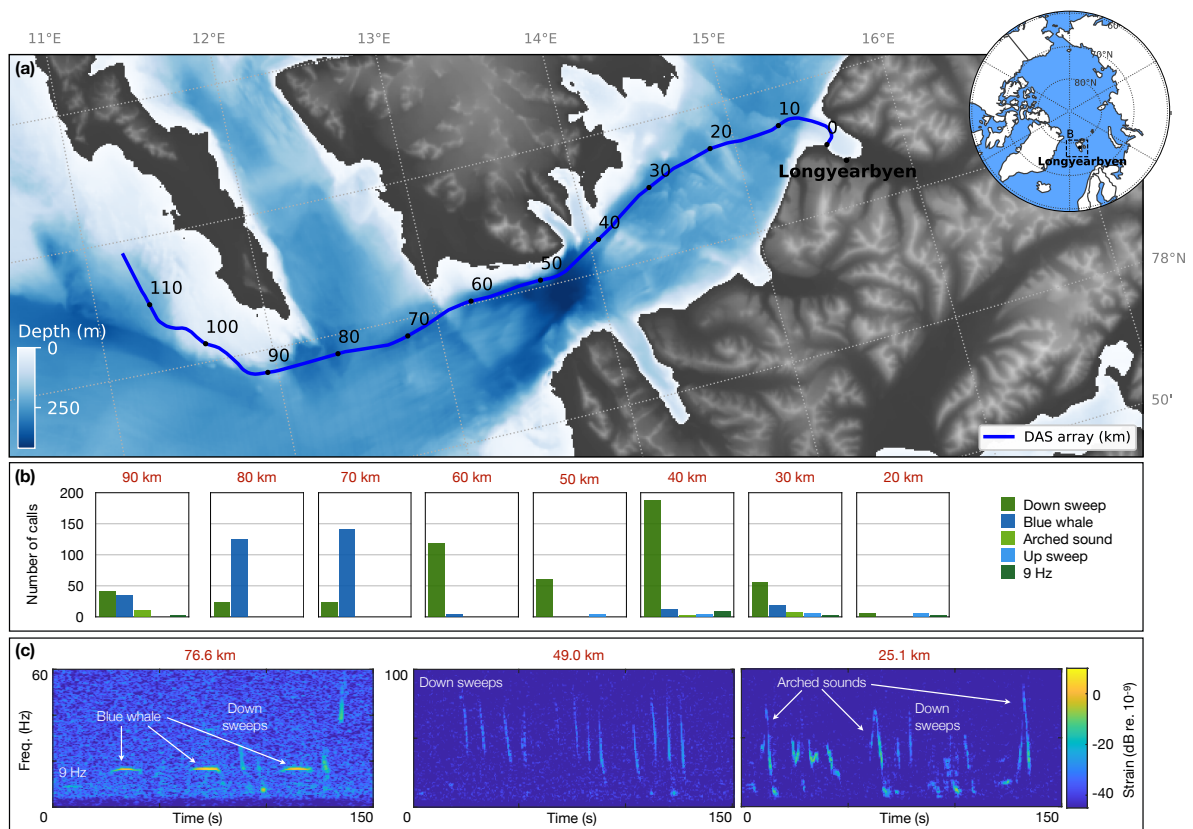


Figure 1: **Baleen whale vocalizations detected over the 120 km of the Svalbard underwater distributed acoustic sensing (DAS) array.** (a) The DAS is trenched on the seafloor of Isfjorden out to the open sea, bypassing the South of Prins Karls Forland in Svalbard, Norway. The interrogator end of the fiber is located on shore in Longyearbyen, recording data with a spatial sampling of 4.08 m at a sampling frequency of  $f_s = 645.16$  Hz between June 23<sup>rd</sup> and August 5<sup>th</sup>, 2020. Number (b) and examples (c) representative of the diversity of baleen whale vocalizations detected along the DAS during the entire recording period. Associated sounds are available in supplementary material Audio S1-S3.

In this experiment, 120 km of fiber were converted into a DAS array, heading out the open ocean from Longyearbyen, through Isfjorden. We used light pulses of 1550 nm free-space wavelength with a duration of 100  $\mu$ s to sample 30000 channels with 4.08 m spacing, covering more than 120 km. The gauge length

108 used was 8.16 m. The signal strength decays along the cable such that the returned signal strength from  
109 100 km is  $\simeq -40$  dB with respect to 1 km. Data is streamed from Svalbard to NTNU in near-real-time  
110 via the Uninett network by using the 1 Gbit/s network interface on the Alcatel interrogator. The DAS  
111 data was continuously sampled over 44 days, between June 23<sup>rd</sup> and August 5<sup>th</sup>, 2020 and streamed over  
112 Uninett’s research network to NTNU in Trondheim, where they were recorded at 645.16 Hz, providing  
113 just over 300 Hz of bandwidth. In the remainder of the article, we refer to the distance along the FO  
114 cable from shore as simply *distance*, as illustrated on Fig. 1. Due to the nature of the coupling of acoustic  
115 stress to FO cable strain, the FO cable has a sensitivity that varies with the gauge length, the frequency  
116 and the angle of arrival between the sound source and the receivers. A notch in the impulse response of  
117 the fiber can be observed for perpendicular arrivals [50].

## 118 2.2 Acoustic Data Analysis

119 A sparse visual and aural inspection of the data revealed the presence of different known baleen whale  
120 low-frequency signatures along the fiber (Fig. 1 (b&c) - Supplementary Audio S1-S3). Of the 832  
121 annotated calls, we identified 38% as North Atlantic blue whale stereotyped signals (AB call, peak  
122 frequency at 16.9 Hz; arched sounds, 9-Hz call) conforming to previous call descriptions [34]. They were  
123 recorded during the entire recording period with a higher number of calls detected after 20200723. In  
124 four instances, sightings from whale-watching tours confirmed the presence of a blue whale in the area.  
125 Down-sweeps (peak frequency  $45 \pm 15$  Hz, average duration  $5.4 \pm 2.4$  s) were the most common calls  
126 (60% of the annotations) and can be attributed to blue whales (D-calls), fin whales (D-calls or pulses),  
127 but also sei whales [38, 40, 52]. Note that the detection range (maximum distance at which a call can  
128 be detected) is frequency-dependent and vary between a 2-5 km cross-line distance from the fiber.

129 Blue whale low frequency stereotyped calls were mostly recorded outside Isfjorden, between 70-90 km  
130 while non-stereotyped down-sweeps were detected in higher numbers in the more sheltered waters of the  
131 fjord. The former have been associated with male vocal behavior while the latter can be produced by  
132 all male, females and calves and have been associated with group social or foraging contexts [39]. The  
133 spatial distribution of these two call types indicates potential variation in habitat use in the monitored  
134 area. The call abundance has good overlap with sighting-based models that demonstrate the increasing  
135 importance of Isfjord as habitat for large baleen whales in Svalbard [49].

136 The spatially distributed observations provided by DAS add a new dimension to the previous (and  
137 ongoing) passive acoustic monitoring of baleen whales in Western Svalbard [2], highlighting potential  
138 variations at an unprecedented scale. However, in regard to the amount of data recorded i.e., almost  
139 7 To a day during our experiment, there is a need for big-data processing methods to scan through,  
140 detect and classify vocalizations and improve species identification especially in heterogeneous call types  
141 such as down-sweeps [40]. Resorting in occupation and presence maps to communicate with stakeholders

142 to mitigate baleen whale exposure to anthropogenic activities.

### 143 2.3 Changing Perspectives: from Single Point to Distributed Sensing

144 One of the advantages of distributed acoustic sensing in comparison to typical single-point sensing is  
 145 that it provides a continuity of measurement in both time and space, which requires "new" represen-  
 146 tation of the data. A common representation in the geophysical community is to use spatio-temporal  
 147 representation or  $f$ - $x$  plots, showing variations in the strain along the FO cable [48].

148 The low-frequency whale vocalizations ( $< 100$  Hz) are transient acoustic signals emitted in the first  
 149 tens of meter of the water column and observed on a very long array, the Svalbard DAS FO cable, that  
 150 is trenched in the bottom of fairly shallow water  $< 400$  m. Therefore, signals will be received only on  
 151 limited portions of the array, with time delays corresponding to the difference of travel times between  
 152 the source and the many receivers (channels). These time delays are inherent to the source-receivers  
 153 configuration and reveal the position of the source.

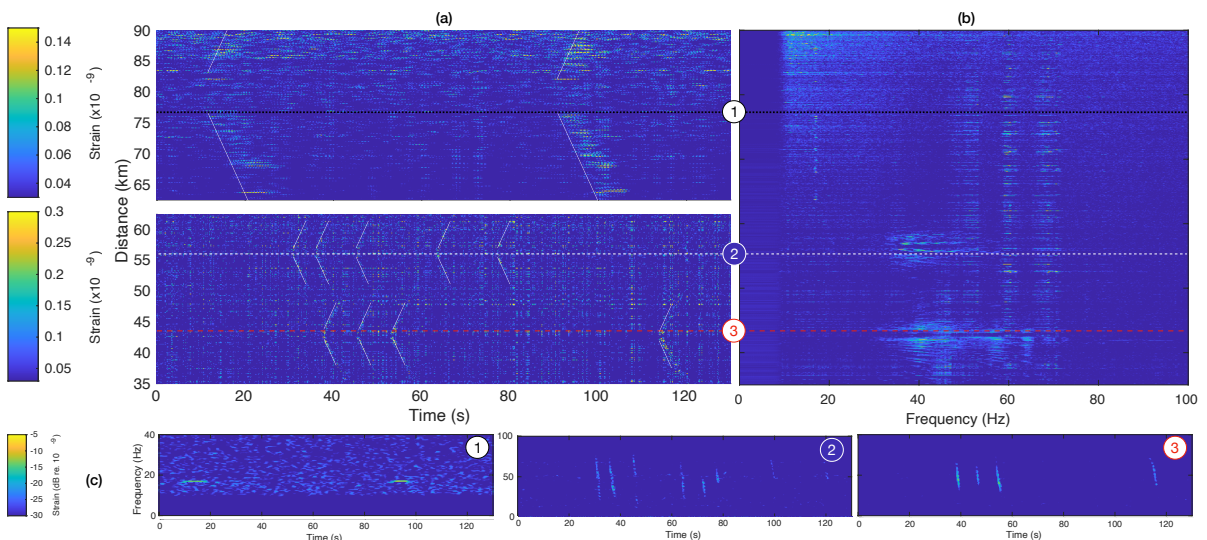


Figure 2: **Vocalizing baleen whales recorded simultaneously at three different locations along the Svalbard fiber optic DAS array.** (a) Spatio-temporal ( $t$ - $x$ ), (b) Spatio-spectral ( $f$ - $x$ ) and (c) Spectro-temporal (spectrogram) representations of a 130 s-long portion of recording from 20200627 at 052440UTC, between 35-90 km of fiber. Each whale position (around 76.5 km, 57.5 km and 44.2 km) is given a number between 1-3, to facilitate between panel associations.

154 Fig. 2 present 180 s of recording on 20200627 at 052440UTC, between 35 and 90 km of the Svalbard  
 155 DAS FO cable. It reveals the presence of at least 3 individuals at different locations along the cable,  
 156 indicated by the dashed lines and numbers. Fig. 2 (a) is a spatio-temporal representation of the strain  
 157 measured along the FO cable, in absolute value and separated around the mouth of the fjord at 62.25 km.  
 158 To enhance the contrast, the signal out of the fjord (62.5 – 90 km) is band-pass filtered in the frequency  
 159 domain between  $[16.7 - 17.2]$  Hz in (a), highlighting the contribution of North Atlantic Blue whale

160 stereotyped signals while it is bandpass-filtered between [30 – 43] Hz to enhance down-sweeps inside the  
 161 fjord (35 – 62.5 km). Spatio-temporal representations highlight the time delays on the received signals  
 162 as hyperbolic wavefront arrivals, whose apex indicate the point on the FO cable closest to the source.  
 163 Lines with a 1500 m/s slope are added to (a) to highlight the received signals. For example a 16.9 Hz  
 164 North-Atlantic blue whale signal is received on all represented channels outside the fjord (a), on more  
 165 than 27 km. The apex indicates that the vocalizing individual is closest to channels at  $\simeq 77$  km. The  
 166 received strain amplitude decay is not constant along the fiber which can be interpreted as (1) DAS  
 167 directivity & coupling between the fiber and seafloor [32, 50], (2) Coherent interferences in the wavefield  
 168 due to a near-surface source (Lloyd’s mirror effect) [10, 11], (3) Upward refracting trends in arctic waters  
 169 sound propagation, with potential shadow zones [24]. In the fjord, the down-sweeps are recorded over  
 170 more than  $\simeq 5$  km around the apexes, indicating two distinct vocalizing positions around 57 and 44 km.  
 171 Fig. 2 (c) are spectrograms of the strain content recorded at 76.54, 57.46 and 44.22 km (Distances  
 172 represented by the dashed lines form matching numbers), averaged over 2 juxtaposed channels (4.08 m  
 173 apart) for noise removal and displayed in dB re.  $10^{-9}$ . Channels for computing the spectrograms (c-d)  
 174 are chosen near to the apex to maximize the received amplitude.

175 Different features are considered to identify the calling species such as the rhythmic or inter-call  
 176 intervals, the intensity or received levels, the contours in the time-frequency domain. However, for  
 177 baleen whales, a decisive characteristics is the spectral content of the signal [33, 56]. We therefore  
 178 propose a spatio-spectral representation of the DAS recordings or  $f$ - $x$  plot, as employed in [44], to show  
 179 the spectral signature and its evolution against the distance. An animation, showing the successive  
 180 2-s  $f$ - $x$  plots is available in supplementary material Video S4 while the integrated representation, over  
 181 the 130 s of recording is displayed in Fig. 2(b) with a time window duration of 2-s and 4096 samples  
 182 fast Fourier transform, resulting in a  $f$ - $x$  matrix with a frequency resolution of 0.16 Hz. For the three  
 183 distances along the FO cable where signals were emitted, the measured bandwidth gives an indication  
 184 on the species: for example the clearly tonal signals around 70 km can be easily identified as Blue whale  
 185 stereotyped call. In the two other locations, they cover a wider band, between 35 – 60 Hz around 57 km  
 186 (whale 2) and wider 30 – 70 Hz around 42 km (whale 3). The received signals also show pattern of  
 187 multi-path coherent interferences (e.g., notches on signals coming from whale 2), modulated by the FO  
 188 cable reception sensitivity null.

189 Fig. 2 reveals the full potential of DAS: it can simultaneously record vocalizing individuals over tens  
 190 of kilometers from a protected fjord area out to the open Ocean, despite varying noise conditions. In  
 191 addition to the change of environment, the increase of background noise along the length of the FO cable  
 192 is due to the attenuation of the optical interrogation pulses. It can also be the effect of changes in the  
 193 coupling between the FO cable and the seafloor [32]. For quality and sensitivity assessment, calibration  
 194 hydrophones could be temporarily installed close to the DAS array. It would enable the estimation of

195 the seafloor’s young modulus and the conversion of the measured strain into acoustic pressure, providing  
 196 regional scale calibrated measurement of ambient sounds. The spatial distribution inherent to DAS also  
 197 opens localization and near-field beamforming possibilities (Sec. 2.4).

## 198 2.4 Localization, Tracking and Beamforming

199 The localization problem is seen as an optimization process, that aims to find the best match between  
 200 measured and theoretical time difference of arrivals (TDOA), estimated for different source position  
 201 (varying closest FO channel and range). Successive positions are linearized for individual tracking and the  
 202 time delay information is used for near-field beamforming. The localization, tracking and beamforming  
 203 method is illustrated on Fig. 3, using a long (more than 10 min) recording with noticeable movement  
 204 of a blue whale.  $t$ - $x$  plots of portion of the recording containing calls and corresponding beamformed  
 205 signals are represented. The white line indicates the variation of the position of the whale, along the FO  
 206 cable ( $x_w$ ) in time, moving from 86.4 to 87.5 km with an apparent speed of 5.4 km/h. The estimation  
 207 of the range was not as precise as  $x_w$ , with a maximum of 700 m and the closest calls emitted (between  
 208 420 – 520 s) within a  $\simeq 100$  m range. Considering the few number of points, no specific trend emerged  
 209 so the beamforming is set for a 200 m range. The resulting spectrogram shows a combination of singular  
 stereotyped unit and D calls, emitted in series, likely from the same animal.

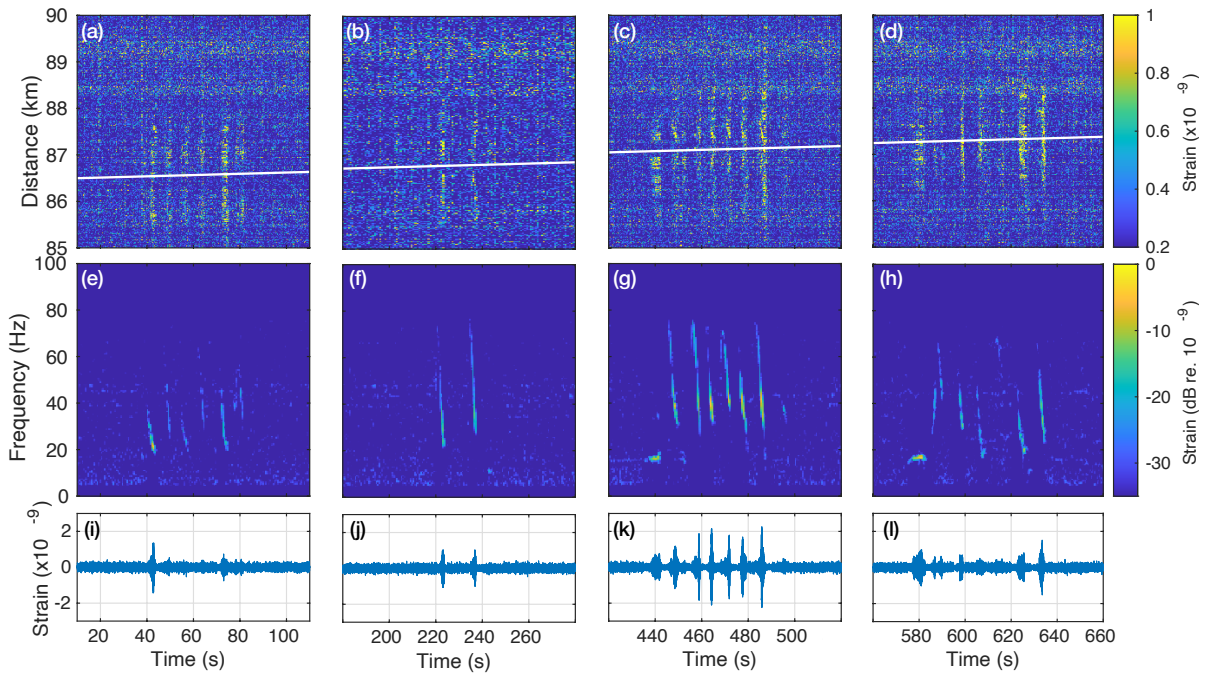


Figure 3: **Tracking and beamforming of series of blue whale calls recorded with a moveout on the Svalbard DAS array.** (a-d) Spatio-temporal ( $t$ - $x$ ) representations of the recorded observation where the white line indicate the tracking of the apex, beamformed signals’ spectrogram (e-h) and waveforms (i-l), displayed as successive 100s-long windows. The audio associated to (c;g;k) is available in supplementary material Audio S5.

210

211 The estimated swim speed of 5.4 km/h is a minimum as the true value increases with the angle between

212 the FO cable and the whale’s trajectory. It is in the bounds of transiting swim speeds reported for blue  
213 whales on feeding grounds, between 2 – 8 km/h[4, 22], and consistent with the behaviors associated to  
214 stereotyped singular unit and D-call vocal production [39].

215 The example on Fig. 3 demonstrates that whales passing over or near a FO cable can be detected and  
216 tracked. The information can subsequently be used, e.g., for counting individuals. Refining the range  
217 estimation will increase the resolution of the localization process but note that locally, FO cables are  
218 laid on the seafloor in straight lines, introducing a left/right ambiguity. At the experiment location, this  
219 issue could be solved by instrumenting another already-installed FO cable running parallel to the used  
220 FO cable, only a couple of kilometers away. More generally, localization improvements require a ground  
221 truth to calibrate and test algorithms. One option is to train them using ship acoustic signals and their  
222 automatic identification system (AIS) position [29, 44]. However, ship signals are continuous while whale  
223 calls are transient, which requires a different initial processing step. Another option is to use acoustic  
224 bio-logging with Global Positioning System (GPS) to combine rich information from calling individuals  
225 and their behavior to DAS observations [30, 39]. Fig. 3 also shows that the high SNR gain available from  
226 extended aperture array processing can be used to construct high-quality audio waveforms (e.g., Audio  
227 S5), which can be further use e.g. for subsurface exploration (Sec. 2.5).

## 228 2.5 Subsurface Exploration

229 Recent work demonstrated that recordings of fin whale vocalizations by seabed vibration sensors con-  
230 tain seismic responses to subsurface geologic structures [28]. The fin whale song produced by males is  
231 composed by series of repeated short and low frequency pulses that share similarities with airgun blasts  
232 [13, 55] and when produced at different locations (e.g., while traveling) in the vicinity of a single sensor,  
233 they can be used to for a common receiver song gather [28]. Concurrently, DAS has demonstrated its  
234 ability to produce seismic images of the subsurface geologic structures using conventional sources [50].

235 Fig. 4 displays correlated seismic profiles (a-b) and associated received interference pattern introduced  
236 by the sea surface (c-d; Lloyd’s mirror effect [11]) obtained from two blue whale D-calls one inside  
237 Isfjorden (a-c) around 25 km of FO cable (Fig. 1 (c), last call) and the other around 87 km of FO cable  
238 (at 458 s on Fig. 3) in the passage between the mouth of the fjord and Prins Karls Forland named  
239 Forlandsundet Graben. The water depth at both location is  $\simeq 260$  m explaining similar first arrival  
240 times (direct waves). The analysis and modeling of the interference patterns (c-d) show a good match  
241 for a  $\simeq 20$  m source depth, in the bounds of reported values for blue whales [30, 39]. Specifically source  
242 depth and range are set at 15 m and 40 m for the call emitted inside the fjord (a) and 20 m and 110 m  
243 outside (b).

244 The correlated call profiles show direct waves, subsurface reflections, and strong water-layer multiple  
245 reflections, annotated on both panels. Comparing the sub-surface reflected waves at the two locations

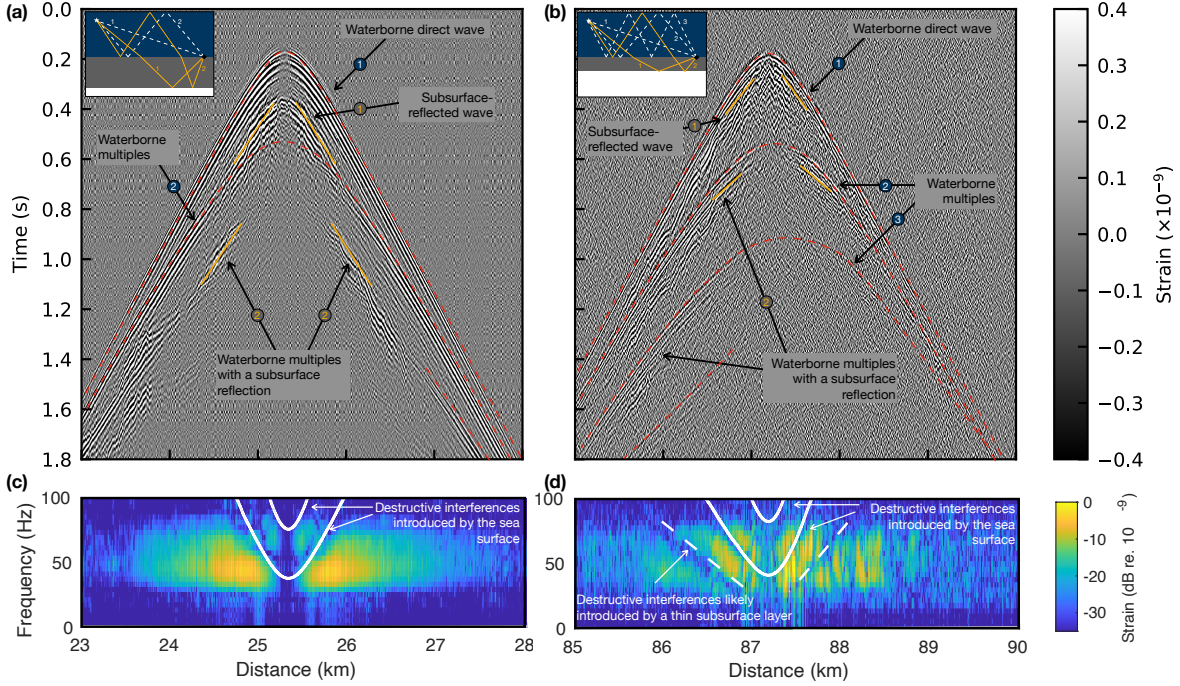


Figure 4: **Correlated seismic profiles from blue whale non-stereotyped calls.** Analysis a D-call (a;c) inside (last from Fig. 1(c), 25.1km)) and (b;d) outside (at 458 s on Fig. 3) Isfjorden. (a-b) correlated seismic profiles at different locations. Key seismic events are highlighted and described by schematic Earth's models in the insets. Observed and modeled interference patterns generated by (c) the sea surface (d) the sea surface and a thin sub-surface layer.

246 shows longer travel times in Isfjorden (a) than in Forlandsundet Garben (b), indicating a thicker shallow  
 247 sedimentary rock layer in the fjord (see insets). The short-time subsurface reflections on the thinner layer  
 248 of Forlandsundet Garben occur in the interference analysis window (110 ms), introducing additional lower  
 249 frequency interference notches in (d). Two (a) and three (b) waterborne multiples are visible in the call  
 250 profiles, indicating a higher stiffness of the seafloor in Forlandsundet Garben due to different surface  
 251 geology, matching traditionally-obtained subsurface structural models [7, Fig. 5f] [3, 8] and reference  
 252 seismic images [46, Fig. 47] for the area. Note that the subsurface primary reflection events observed in  
 253 these two call profiles are reflected shear waves, which are probably corrupted by refracted shear waves  
 254 from the same interfaces.

255 Fig. 4 demonstrates that each whale frequency-modulated call recorded by DAS can provide conven-  
 256 tional seismic records for subsurface exploration. This example goes further than the proposal made by  
 257 [28] to use stereotyped fin whale male song and uses non-stereotyped vocalizations such as D-calls, pro-  
 258 duced by all individuals in various baleen whales species [39, 40]. We show that in areas where vocalizing  
 259 baleen whales and DAS overlap, seismic exploration could be replaced - at least partially - by an entirely  
 260 passive method keeping the environment and ecosystems undisturbed and unharmed. Therefore, DAS  
 261 could reduce human activities and anthropogenic stressors such as noise in the oceans.

## 3 Conclusions

More than 1.2 million km of fiber-optic cables are installed all over the world’s oceans. We demonstrate through this work that, with tailored filtering, analyzing, and visualizing methods, DAS can provide data for all passive acoustic monitoring applications with an unequalled and unprecedented spatial coverage and resolution. As a result, we are on the brink of a revolution.

However, to reach its fullest potential, DAS demands big data handling methods and real-time processing along with efficient ways to scan through fast computed time-space-frequency representation of the data (the 120 km of FO cable sampled for this work generated 7 TB of data a day), process and detect potential signals of interest. Besides, while there is a trade-off between the length of cable converted to DAS and the sampling frequency, it is possible to monitor only a specific section of interest at higher frequencies, e.g., 9 km with a sampling frequency of 10 kHz, widening the variety of species recorded. In the future, DAS could be set with an adaptive frequency span: a relatively lower range for long-term and large-scale ”standby” and a wider frequency coverage upon the detection of a signal of interest in a designated zone. Thus, DAS can comprehensively monitor ecosystems with unprecedented spatial coverage, contributing to filling up the worldwide monitoring gaps for conservation.

The final example demonstrated that the spatial resolution of DAS enables the generalization of unique passive acoustics applications such as subsurface exploration using whale calls and could contribute to reducing anthropogenic stressors on marine life. Therefore, DAS can help us study, preserve and protect the oceans.

## 4 Methods

### 4.1 Acoustic Analysis

The DAS-recorded data was exported as audio files every 10 km of the fiber, starting from 20 km offshore. The analysis was conducted using spectrograms at all locations in parallel and for the 42 days of recording by two independent and experimented analysts (H.J.K. & L.B.) using Raven Pro v1.6.1 [25]. Any potential whale call was then annotated with with a time-frequency contour and given a label.

### 4.2 Spatio-temporal Representation Conditioning

The data matrices (amplitude versus time and distance) are pre-processed to improve the Signal to Noise Ratio (SNR) and contrast in the spatio-temporal representation. In the following examples, the signal is first band-pass filtered before the application of a  $3 \times 3$  symmetrical 2D median filter (resolution of 12 m/4.65 ms). Absolute values are used in the  $t-x$  representation. The median value is successively subtracted from each time and space sample of the absolute amplitude (median subtracted from each

293 row and column).

### 294 4.3 Spatio-spectral Representation

295 The recordings are analyzed with a time window duration relevant to the minimum duration of whale  
296 calls. The frequency content is then calculated on each channel by a fast Fourier transform, constructing  
297 the  $f$ - $x$  matrix. The median value is subtracted from each row and column for noise reduction. It is  
298 possible to generate an image for each time window. For a representation integrated over a longer time  
299 period, we used for each point of the  $f$ - $x$  grid the difference between its maximum and average value in  
300 time.

### 301 4.4 Localization, Tracking and Beamforming

DAS receivers at the positions  $R\{x, r = 0, z\}$  and whale position is at  $S\{x = x_w, r = r_w, z = z_w\}$  where  
 $x$  is the position along the FO cable,  $r$  the cross-line range from the FO cable,  $z$  the depth and the  
subscript  $w$  stands for the whale. A grid of potential whale positions along the FO cable  $x_n$  and ranges  
 $r_m$  are established for the optimization problem, assuming a fixed calling depth  $z_w = 30$  m [10, 30]. The  
source position is estimated by finding the theoretical TDOA that matches best the observed TDOA  
between all receivers an arbitrary chosen reference receiver position  $R_0\{x_0, r = 0, z_0\}$  such as

$$\text{TDOA}_{m,n} = \frac{h_{n,m} - h_{0,m}}{c} \quad (1)$$

302 with  $c = 1500$  m/s the constant sound speed,  $h_{n,m} = \sqrt{|x - x_n|^2 + r_m^2 + |z - z_w|^2}$  where  $|x - x_n|^2$   
303 represents the distance between each receiver position and the tested position along the FO cable and  
304  $h_{0,m}$  is  $h_{n,m}$  but for the reference  $R_0$ . The search grid used has a resolution of 50 m in  $x$ , within  
305 predefined 5 km bound around observed signal apexes ( $[85 - 90]$  km) and a 20 m resolution in ranges,  
306 from  $[0 - 4]$  km. Note, that the water depth is deeper than 300 m before 87 m and about 180 m at  
307 90 km.

308 The  $t$ - $x$  observation is sectioned in 5-s windows and band-pass filtered  $[5 - 80]$ . The 5-s-duration of  
309 the window allows to integrate the calculation over a period that is in the same order as the observed  
310 signals and, to cover potential time delays over the entire observed FO length. In the TDOA the apex  
311 gives information on  $x_w$  while the opening of the hyperbola gives information on  $r_w$ . The TDOA are  
312 estimated for each receiver position as the lags corresponding to the maximum of the cross-correlation  
313 between  $R_0$  and the other receivers. Unrealistic values e.g.  $|\text{TDOA}| \geq \text{observed FO length over } c$  are  
314 discarded along with  $|\text{TDOA}| \leq 5$  ms.

315 The optimization process is performed in 3 steps. First, the initialization cross-correlates measured  
316 and theoretical TDOA, where the maximum outcome initializes  $S\{x = x_w, r = r_w, z = z_w\}$ . The process

317 is ran a second time, after filtering out measurement points that diverge from the initialization fit of  
318 more than the standard deviation of the difference between the theoretical and measured data points.  
319 This second run gives the best  $x_w$ . A third step is added to improve the  $r_w$  estimation by minimizing  
320 the root mean square error between the theoretical and measured points, in a 1 km window around  $x_w$ .

321 To extend the single point localization to tracking, the localization procedure is applied iteratively  
322 to each 5-s window and only  $S\{x = x_w, r = r_w, z = z_w\}$  points with a correlation coefficient higher than  
323 0.85 are kept. The threshold is chosen to differentiate between signal and noise windows.

324 Once  $S\{x = x_w, r = r_w, z = z_w\}$  known, time delays can be compensated to beamform the received  
325 signal. In practice, only the 10 receivers with the most energy are summed-up, to limit the influence of  
326 coherent destructive interferences.

## 327 4.5 Correlated Call Profiles and Interferences Analysis

328 It is possible to use frequency-modulated sweep signals from whales' vocalizations measured by the seabed  
329 DAS array in Svalbard for subsurface exploration. The used D-calls are 4–8 s long down-sweeps, similar  
330 to the seismic signals from vibroseis [12], a commonly used source in land seismic exploration. Therefore,  
331 estimating the emitted signals is necessary to produce interpretable call profiles by cross-correlation with  
332 the recorded calls.

333 Each source signature is extracted from the DAS data using the previously described near-field  
334 beamforming method (stacking after time-delay compensation). The source signature derived from this  
335 method contains coherent interferences introduced by, e.g., the reflection with a change of phase at the  
336 surface, known as the Lloyd's mirror effect [11] or ghost effect. Finally, the interference analysis (Fig. 4)  
337 is performed on a short (110 ms) portion of the time-delay-compensated signal, chosen to include the  
338 waterborne direct arrival and the sea-surface reflection. The source depth is estimated from the frequency  
339 notches associated with the interferences patterns [10, 42] and information on the time of arrival of the  
340 sea-surface reflected wave given by the delay in the source signature autocorrelation.

341 The contribution of the interferences is removed by applying predictive (gapped) deconvolution [45] to  
342 the source signature, based on the estimated time delay information. Finally, to obtain a seismic profile,  
343 the DAS strain data associated with a whale call is cross-correlated with the corresponding deconvolved  
344 source signature.

## 345 Conflict of Interest Statement

346 The authors declare that the research was conducted in the absence of any commercial or financial  
347 relationships that could be construed as a potential conflict of interest.

## 348 **Author Contributions**

349 LB wrote the manuscript, read and approved by all co-authors. LB and HJK conducted the acoustic data  
350 analysis; LB designed and produced most of the results shown in the manuscript, interpreted together  
351 with HJK, ML and JRP. KT and ML produced and wrote about the subsurface exploration results and  
352 interpretation. LB, KT and RAR developed data handling and processing routines. ML, JKB, AH, SEJ,  
353 OS, and FS conceived the experiment, AH and FS collected the DAS data.

## 354 **Funding**

355 LB and HJK are funded by the Research Center for Arctic Petroleum Exploration (ARCEX) partners,  
356 and the Research Council of Norway (Grant No. 228107). KT and RAR are funded by the Geophysics  
357 and Applied Mathematics in Exploration and Safe production Project (GAMES) at NTNU (Research  
358 Council of Norway; Grant No. 294404). ML, JRP, and SEJ receive research funding from the Centre  
359 for Geophysical Forecasting (CGF) at NTNU, sponsored by Grant No. 309960 (Research Council of  
360 Norway). The acquisition of the data was financed by ARCEX and GAMES.

## 361 **Acknowledgments**

362 Whale sighting provided by Svalbard Adventures and Henningsen Transport & Guiding.

## 363 **Supplemental Data**

- 364 1. Audio S1; Audio associated to the series of stereotyped North Atlantic blue whale calls and down-  
365 sweeps represented on Fig. 1(c) at 76.6 km, sped up 3.5 times;
- 366 2. Audio S2; Audio associated to the series of down sweeps represented on Fig. 1(c), sped up 3.5  
367 times;
- 368 3. Audio S3; Audio associated to the series of non-stereotyped arched sounds and down sweeps rep-  
369 resented on Fig. 1(c) 25.1 km, sped up 3.5 times;
- 370 4. Video S4; Animation showing the successive 2-s  $f$ - $x$  plots used to construct the integrated repre-  
371 sentation of Fig. 2(b).
- 372 5. Audio S5; High-quality beamformed audio of the blue whale stereotyped and D-calls represented  
373 on Fig. 2.4(c;g;k), sped up 3.5 times.

## 374 Data Availability Statement

375 The DAS-recorded spatio-temporal strain data supporting this analysis is available at [https://doi.](https://doi.org/10.5281/zenodo.5823343)  
376 [org/10.5281/zenodo.5823343](https://doi.org/10.5281/zenodo.5823343) [9].

## 377 References

- 378 [1] Heidi Ahonen, Kathleen M Stafford, Laura de Steur, Christian Lydersen, Øystein Wiig, and Kit M  
379 Kovacs. The underwater soundscape in western fram strait: Breeding ground of spitsbergen's  
380 endangered bowhead whales. *Marine pollution bulletin*, 123(1-2):97–112, 2017.
- 381 [2] Heidi Ahonen, Kathleen M Stafford, Christian Lydersen, Catherine L Berchok, Sue E Moore, and  
382 Kit M Kovacs. Interannual variability in acoustic detection of blue and fin whale calls in the  
383 northeast atlantic high arctic between 2008 and 2018. *Endangered Species Research*, 45:209–224,  
384 2021. doi:10.3354/esr01132.
- 385 [3] Abrar Asghar. Processing and interpretation of multichannel seismic data from Isfjorden, Svalbard.  
386 Master's thesis, The University of Bergen, 2011. URL <https://hdl.handle.net/1956/5760>.
- 387 [4] Helen Bailey, Bruce R Mate, Daniel M Palacios, Ladd Irvine, Steven J Bograd, and Daniel P Costa.  
388 Behavioural estimation of blue whale movements in the northeast pacific from state-space model  
389 analysis of satellite tracks. *Endangered Species Research*, 10:93–106, 2009. doi:10.3354/esr00239.
- 390 [5] John L Bannister. Baleen whales (mysticeti). In *Encyclopedia of Marine Mammals*, pages 62–69.  
391 Elsevier, 2018. doi:10.1016/B978-0-12-804327-1.00058-3.
- 392 [6] Mark F. Baumgartner, Kathleen M. Stafford, and G. Latha. Near real-time underwater passive  
393 acoustic monitoring of natural and anthropogenic sounds. In R. Venkatesan, Amit Tandon, Eric  
394 D'Asaro, and M. A. Atmanand, editors, *Observing the Oceans in Real Time*, pages 203–226, Cham,  
395 2018. Springer International Publishing. doi:10.1007/978-3-319-66493-4\_10.
- 396 [7] Maria Blinova, Rune Thorsen, Rolf Mjelde, and Jan Inge Faleide. Structure and evolution of the  
397 Bellsund Graben between Forlandsundet and Bellsund (Spitsbergen) based on marine seismic data.  
398 *Norwegian Journal of Geology*, 89:215–228, 2009. ISSN 029-196X. URL [https://hdl.handle.net/](https://hdl.handle.net/1956/5861)  
399 [1956/5861](https://hdl.handle.net/1956/5861).
- 400 [8] Maria Blinova, Jan Inge Faleide, Roy H. Gabrielsen, and Rolf Mjelde. Seafloor expression and  
401 shallow structure of a fold-and-thrust system, Isfjorden, west Spitsbergen. *Polar Research*, 31:  
402 11209, 2012. doi:10.3402/polar.v31i0.11209.

- 403 [9] L. Bouffaut and K. Taweessintananon. Das4whale: Svalbard distributed acoustic sensing dataset for  
404 baleen whale monitoring, 2022. URL <https://doi.org/10.5281/zenodo.5823343>.
- 405 [10] Léa Bouffaut, Martin Landrø, and John R Potter. Source level and vocalizing depth estimation of  
406 two blue whale subspecies in the western indian ocean from single sensor observations. *The Journal*  
407 *of the Acoustical Society of America*, 149(6):4422–4436, 2021. doi:10.1121/10.0005281.
- 408 [11] William M Carey. Lloyd’s mirror-image interference effects. *Acoust. Today*, 5(2):14–20, 2009. doi:  
409 10.1121/1.3182842.
- 410 [12] John M. Crawford, William E. N. Doty, and Milford R. Lee. Continuous signal seismograph. *Geo-*  
411 *physics*, 25(1):95–105, 1960. doi:10.1190/1.1438707.
- 412 [13] Donald A Croll, Alejandro Acevedo-Gutiérrez, Bernie R Tershy, and Jorge Urbán-Ramírez. The  
413 diving behavior of blue and fin whales: is dive duration shorter than expected based on oxygen  
414 stores? *Comparative Biochemistry and Physiology Part A: Molecular & Integrative Physiology*, 129  
415 (4):797–809, 2001. doi:10.1016/S1095-6433(01)00348-8.
- 416 [14] Brian Culshaw and Alan Kersey. Fiber-optic sensing: A historical perspective. *Journal of lightwave*  
417 *technology*, 26(9):1064–1078, 2008.
- 418 [15] Thomas M. Daley, Barry M. Freifeld, Jonathan Ajo-Franklin, Shan Dou, Roman Pevzner, Valeriya  
419 Shulakova, Sudhendu Kashikar, Douglas E. Miller, Julia Goetz, Jan Henninges, and Stefan Lueth.  
420 Field testing of fiber-optic distributed acoustic sensing (DAS) for subsurface seismic monitoring. *The*  
421 *Leading Edge*, 32(6):699–706, 2013. ISSN 1070-485X, 1938-3789. doi:10.1190/tle32060699.1.
- 422 [16] Victor M Eguíluz, Juan Fernández-Gracia, Xabier Irigoien, and Carlos M Duarte. A quan-  
423 titative assessment of arctic shipping in 2010–2014. *Scientific reports*, 6(1):1–6, 2016. doi:  
424 10.1038/srep30682.
- 425 [17] Alex Goertz and Andreas Wuestefeld. Real-time passive monitoring with a fibre-optic ocean bottom  
426 array. *First Break*, 36(4):55–61, 2018. doi:10.3997/1365-2397.n0083.
- 427 [18] Charmain D Hamilton, Christian Lydersen, Jon Aars, Martin Biuw, Andrei N Boltunov, Erik W  
428 Born, Rune Dietz, Lars P Folkow, Dmitri M Glazov, Tore Haug, et al. Marine mammal hotspots  
429 in the greenland and barents seas. *Marine Ecology Progress Series*, 659:3–28, 2021. doi:10.3354/  
430 meps13584.
- 431 [19] Arthur H Hartog. *An introduction to distributed optical fibre sensors*. CRC press, 2017.
- 432 [20] Arthur H Hartog, Mohammad Belal, and Michael A Clare. Advances in distributed fiber-optic  
433 sensing for monitoring marine infrastructure, measuring the deep ocean, and quantifying the risks

- 434 posed by seafloor hazards. *Marine Technology Society Journal*, 52(5):58–73, 2018. doi:doi.org/  
435 10.4031/MTSJ.52.5.7.
- 436 [21] Bruce M Howe, Jennifer Miksis-Olds, Eric Rehm, Hanne Sagen, Peter F Worcester, and Georgios  
437 Haralabus. Observing the oceans acoustically. *Frontiers in Marine Science*, 6:426, 2019. doi:  
438 10.3389/fmars.2019.00426.
- 439 [22] Rodrigo Hucke-Gaete, Luis Bedriñana-Romano, Francisco A Vidali, Jorge E Ruiz, Juan Pablo Torres-  
440 Florez, and Alexandre N Zerbini. From chilean patagonia to galapagos, ecuador: novel insights  
441 on blue whale migratory pathways along the eastern south pacific. *PeerJ*, 6:e4695, 2018. doi:  
442 10.7717/peerj.4695.
- 443 [23] IUCN 2021. The IUCN red list of threatened species, Version 2021-2.
- 444 [24] Finn B Jensen, William A Kuperman, Michael B Porter, and Henrik Schmidt. *Computational Ocean*  
445 *Acoustics*. Springer Science & Business Media, 2011. doi:10.1007/978-1-4417-8678-8.
- 446 [25] K. Lisa Yang Center for Conservation Bioacoustics. Raven pro: Interactive sound analysis software  
447 (version 1.6.1), 2019. URL <http://ravensoundsoftware.com/>.
- 448 [26] Holger Klinck, Sharon L Niekirk, David K Mellinger, Karolin Klinck, Haruyoshi Matsumoto, and  
449 Robert P Dziak. Seasonal presence of cetaceans and ambient noise levels in polar waters of the  
450 north atlantic. *The Journal of the Acoustical Society of America*, 132(3):EL176–EL181, 2012. doi:  
451 10.1121/1.4740226.
- 452 [27] Katie A Kowarski and Hilary Moors-Murphy. A review of big data analysis methods for baleen  
453 whale passive acoustic monitoring. *Marine Mammal Science*, 37(2):652–673, 2021. doi:10.1111/  
454 mms.12758.
- 455 [28] Václav M Kuna and John L Nábělek. Seismic crustal imaging using fin whale songs. *Science*, 371  
456 (6530):731–735, 2021. doi:10.1126/science.abf3962.
- 457 [29] Martin Landrø, Léa Bouffaut, Hannah Joy Kriesell, John Robert Potter, Robin André  
458 Rørstadbotnen, Kittinat Taweasantanon, Ståle Emil Johansen, Jan Kristoffer Brenne, Aksel  
459 Haukanes, Olaf Schjelderup, and et al. Title: Sensing whales, storms, ships and earthquakes  
460 using an arctic fibre- optic cable. *Earth and Space Science Open Archive*, page 39, 2021. doi:  
461 10.1002/essoar.10507855.1. URL <https://doi.org/10.1002/essoar.10507855.1>.
- 462 [30] Leah A Lewis, John Calambokidis, Alison K Stimpert, James Fahlbusch, Ari S Friedlaender,  
463 Megan F McKenna, Sarah L Mesnick, Erin M Oleson, Brandon L Southall, Angela R Szescioraka,  
464 et al. Context-dependent variability in blue whale acoustic behaviour. *Royal Society open science*,  
465 5(8):180241, 2018. doi:10.1098/rsos.180241.

- 466 [31] Christian Lydersen, Jade Vacquié-Garcia, Mads Peter Heide-Jørgensen, Nils Øien, Christophe  
467 Guinet, and Kit M Kovacs. Autumn movements of fin whales (*balaenoptera physalus*) from sval-  
468 bard, norway, revealed by satellite tracking. *Scientific reports*, 10(1):1–13, 2020. doi:10.1038/  
469 s41598-020-73996-z.
- 470 [32] Hiroyuki Matsumoto, Eiichiro Araki, Toshinori Kimura, Gou Fujie, Kazuya Shiraishi, Takashi Tone-  
471 gawa, Koichiro Obana, Ryuta Arai, Yuka Kaiho, Yasuyuki Nakamura, Takashi Yokobiki, Shuichi  
472 Kodaira, Narumi Takahashi, Robert Ellwood, Victor Yartsev, and Martin Karrenbach. Detection  
473 of hydroacoustic signals on a fiber-optic submarine cable. *Scientific Reports*, 11(1):2797, 2021.  
474 doi:10.1038/s41598-021-82093-8.
- 475 [33] M. A. McDonald, S. L. Mesnick, and J. A. Hildebrand. Biogeographic characterization of blue whale  
476 song worldwide: Using song to identify populations. *Journal of Cetacean Research and Management*,  
477 8(1):55–65, 2006.
- 478 [34] David K Mellinger and Christopher W Clark. Blue whale (*balaenoptera musculus*) sounds from the  
479 North Atlantic. *J. Acoust. Soc. Am.*, 114(2):1108–1119, 2003.
- 480 [35] David K Mellinger, Kathleen M Stafford, Sue E Moore, Robert P Dziak, and Haru Matsumoto. An  
481 overview of fixed passive acoustic observation methods for cetaceans. *Oceanography*, 20(4):36–45,  
482 2007.
- 483 [36] Sue E Moore, Tore Haug, Gísli A Víkingsson, and Garry B Stenson. Baleen whale ecology in arctic  
484 and subarctic seas in an era of rapid habitat alteration. *Progress in Oceanography*, 176:102118, 2019.  
485 doi:10.1016/j.pocean.2019.05.010.
- 486 [37] Adolf KY Ng, Jonathan Andrews, David Babb, Yufeng Lin, and Austin Becker. Implications of  
487 climate change for shipping: Opening the arctic seas. *Wiley Interdisciplinary Reviews: Climate*  
488 *Change*, 9(2):e507, 2018.
- 489 [38] Sharon L Nieukirk, David K Mellinger, Robert P Dziak, Haru Matsumoto, and Holger Klinck. Multi-  
490 year occurrence of sei whale calls in north atlantic polar waters. *The Journal of the Acoustical Society*  
491 *of America*, 147(3):1842–1850, 2020. doi:10.1121/10.0000931.
- 492 [39] Erin M Oleson, John Calambokidis, William C Burgess, Mark A McDonald, Carrie A LeDuc, and  
493 John A Hildebrand. Behavioral context of call production by eastern north pacific blue whales.  
494 *Marine Ecology progress series*, 330:269–284, 2007. doi:10.3354/meps330269.
- 495 [40] Hui Ou, Whitlow WL Au, Sofie Van Parijs, Erin M Oleson, and Shannon Rankin. Discrimination  
496 of frequency-modulated baleen whale downsweep calls with overlapping frequencies. *The Journal of*  
497 *the Acoustical Society of America*, 137(6):3024–3032, 2015. doi:10.1121/1.4919304.

- 498 [41] Tom Parker, Sergey Shatalin, and Mahmoud Farhadiroushan. Distributed acoustic sensing—a new  
499 tool for seismic applications. *First Break*, 32(2), 2014. doi:10.3997/1365-2397.2013034.
- 500 [42] Andreia Pereira, Danielle Harris, Peter Tyack, and Luis Matias. On the use of the lloyd’s mirror  
501 effect to infer the depth of vocalizing fin whales. *J. Acoust. Soc. Am.*, 148(5):3086–3101, 2020.  
502 doi:10.1121/10.0002426.
- 503 [43] Randall R Reeves, Peter J Ewins, Selina Agbayani, Mads Peter Heide-Jørgensen, Kit M Kovacs,  
504 Christian Lydersen, Robert Suydam, Wendy Elliott, Gert Polet, Yvette van Dijk, et al. Distribution  
505 of endemic cetaceans in relation to hydrocarbon development and commercial shipping in a warming  
506 arctic. *Marine Policy*, 44:375–389, 2014. doi:10.1016/j.marpol.2013.10.005.
- 507 [44] Diane Rivet, Benoit de Cacqueray, Anthony Sladen, Aurélien Roques, and Gaëtan Calbris. Prelim-  
508 inary assessment of ship detection and trajectory evaluation using distributed acoustic sensing on  
509 an optical fiber telecom cable. *The Journal of the Acoustical Society of America*, 149(4):2615–2627,  
510 2021. doi:10.1121/10.0004129.
- 511 [45] Enders A Robinson and Sven Treitel. *Digital imaging and deconvolution: The ABCs of seismic*  
512 *exploration and processing*. Society of Exploration Geophysicists, 2008.
- 513 [46] Niklas Wilko Schaaf. Tectono-sedimentary history of the Forlandsundet Graben. Master’s thesis,  
514 University of Oslo, 2018. URL <http://hdl.handle.net/10852/67489>.
- 515 [47] Luca Schenato. A review of distributed fibre optic sensors for geo-hydrological applications. *Applied*  
516 *Sciences*, 7(9):896, 2017. doi:/doi.org/10.3390/app7090896.
- 517 [48] Pravin M Shah and FK Levin. Gross properties of time-distance curves. *Geophysics*, 38(4):643–656,  
518 1973.
- 519 [49] Luke Storrie, Christian Lydersen, Magnus Andersen, Russell B Wynn, and Kit M Kovacs. Deter-  
520 mining the species assemblage and habitat use of cetaceans in the svalbard archipelago, based on  
521 observations from 2002 to 2014. *Polar Research*, 37(1):1463065, 2018. doi:10.1080/17518369.  
522 2018.1463065.
- 523 [50] Kittinat Taweessintananon, Martin Landrø, Jan Kristoffer Brenne, and Aksel Haukanes. Distributed  
524 acoustic sensing for near-surface imaging using submarine telecommunication cable: A case study in  
525 the Trondheimsfjord, Norway. *Geophysics*, 86(5):B303–B320, 2021. doi:10.1190/geo2020-0834.1.
- 526 [51] Peter O Thomas, Randall R Reeves, and Robert L Brownell Jr. Status of the world’s baleen whales.  
527 *Marine Mammal Science*, 32(2):682–734, 2016. doi:10.1111/mms.12281.

- 528 [52] Christopher J Tremblay, Sofie M Van Parijs, and Danielle Cholewiak. 50 to 30-hz triplet and  
529 singlet down sweep vocalizations produced by sei whales (*balaenoptera borealis*) in the western  
530 north atlantic ocean. *The Journal of the Acoustical Society of America*, 145(6):3351–3358, 2019.  
531 doi:10.1121/1.5110713.
- 532 [53] Celine van Weelden, Jared R Towers, and Thijs Bosker. Impacts of climate change on cetaceans  
533 distribution, habitat and migration. *Climate Change Ecology*, page 100009, 2021. doi:10.1016/j.  
534 ecochg.2021.100009.
- 535 [54] Ole Henrik Waagaard, Erlend Rønnekleiv, Aksel Haukanes, Frantz Stabo-Eeg, Dag Thingbø, Stig  
536 Forbord, Svein Erik Aasen, and Jan Kristoffer Brenne. Real-time low noise distributed acoustic  
537 sensing in 171 km low loss fiber. *OSA Continuum*, 4(2):688–701, 2021. doi:10.1364/OSAC.408761.
- 538 [55] William A. Watkins, Peter Tyack, Karen E. Moore, and James E. Bird. The 20-Hz signals of finback  
539 whales (*balaenoptera physalus*). *J. Acoust. Soc. Am.*, 82(6):1901–1912, 1987.
- 540 [56] A Širović, M McDonald, NE Balcazar-Cabrera, S Buchan, S Cerchio, C Clark, G Davis, K Findlay,  
541 G Gagnon, N Kyo, E Leroy, J Miksis-Olds, B Miller, EM Oleson, T Pangerc, Rogers TH, F Samaran,  
542 Y Simard, KM Stafford, D Stevenson, H Sugioka, K Tomish, JS Tripovich, G Truong, I Van Opzee-  
543 land, S Van Parijs, R Yoshida, and RL. Brownell Jr. Blue whale songs worldwide: an update. In  
544 *22nd Biennial Conference of the Biology of Marine Mammals*. Society for Marine Mammalogy, 2017.